NeuroImage: Clinical 5 (2014) 141–151

Contents lists available at ScienceDirect

NeuroImage: Clinical

journal homepage: www.elsevier.com/locate/ynicl

Aberrant error processing in relation to symptom severity in obsessive–compulsive disorder: A multimodal neuroimaging study

Yigal Agam [a,b], Jennifer L. Greenberg [a], Marlisa Isom [a], Martha J. Falkenstein [a], Eric Jenike [a], Sabine Wilhelm [a], Dara S. Manoach [a,b,*]

[a] Department of Psychiatry, Massachusetts General Hospital, Harvard Medical School, Boston, MA, USA
[b] Athinoula A. Martinos Center for Biomedical Imaging, Harvard Medical School, Charlestown, MA, USA

ARTICLE INFO

Article history:
Received 2 December 2013
Received in revised form 2 June 2014
Accepted 7 June 2014
Available online 17 June 2014

Keywords:
OCD
ERN
Anterior cingulate
Default network
Error processing
Multimodal neuroimaging

ABSTRACT

Background: Obsessive–compulsive disorder (OCD) is characterized by maladaptive repetitive behaviors that persist despite feedback. Using multimodal neuroimaging, we tested the hypothesis that this behavioral rigidity reflects impaired use of behavioral outcomes (here, errors) to adaptively adjust responses. We measured both neural responses to errors and adjustments in the subsequent trial to determine whether abnormalities correlate with symptom severity. Since error processing depends on communication between the anterior and the posterior cingulate cortex, we also examined the integrity of the cingulum bundle with diffusion tensor imaging.
Methods: Participants performed the same antisaccade task during functional MRI and electroencephalography sessions. We measured error-related activation of the anterior cingulate cortex (ACC) and the error-related negativity (ERN). We also examined post-error adjustments, indexed by changes in activation of the default network in trials surrounding errors.
Results: OCD patients showed intact error-related ACC activation and ERN, but abnormal adjustments in the post- vs. pre-error trial. Relative to controls, who responded to errors by deactivating the default network, OCD patients showed *increased* default network activation including in the rostral ACC (rACC). Greater rACC activation in the post-error trial correlated with more severe compulsions. Patients also showed increased fractional anisotropy (FA) in the white matter underlying rACC.
Conclusions: Impaired use of behavioral outcomes to adaptively adjust neural responses may contribute to symptoms in OCD. The rACC locus of abnormal adjustment and relations with symptoms suggests difficulty suppressing emotional responses to aversive, unexpected events (e.g., errors). Increased structural connectivity of this paralimbic default network region may contribute to this impairment.

1. Introduction

Obsessive–compulsive disorder (OCD) is characterized by stereotyped and repetitive behaviors that persist despite feedback. These behaviors serve to reduce distress, but are often excessive and not realistically connected to the feared outcome they are intended to prevent. For example, an individual with OCD may feel compelled to repeatedly check that the door is locked despite having just locked the door, 'knowing' that the door is locked, and wanting to stop. In this scenario, the distressing feeling that the door is not locked persists despite clear evidence to the contrary and compels repetitive checking. Such repetitive, maladaptive behaviors may reflect impaired use of feedback about outcomes (e.g., a locked door) to adjust emotional (e.g., distress) and behavioral (e.g., checking) responses. Here, we used multimodal neuroimaging to test the hypothesis that impaired use of outcomes – in this study, errors – to adaptively adjust future responses characterizes OCD and contributes to symptoms. Since error processing involves (*i*) recognizing that an error has occurred and (*ii*) adjusting future responses and since deficits in either of these abilities could contribute to rigid, repetitive behavior, we examined the neural and behavioral markers of each.

We used an antisaccade paradigm to study error processing. Antisaccades require inhibition of the prepotent response of looking towards a suddenly appearing stimulus and the substitution of a gaze in the opposite direction. Antisaccade errors (i.e., looking towards the stimulus) reliably elicit neural and behavioral error markers (Agam et al., 2011; Belopolsky and Kramer, 2006; Endrass et al., 2007; Klein et al., 2007; Nieuwenhuis et al., 2001; Polli et al., 2005). We first investigated whether individuals with OCD show intact error detection as indexed by error self-correction and two extensively characterized and highly reliable neural error markers: the error-related negativity (ERN) as measured by electroencephalography (EEG) and functional

* Corresponding author at: Psychiatric Neuroimaging, Massachusetts General Hospital, 149 13th Street, Room 1.111, Charlestown, MA 02129, USA.
E-mail address: dara@nmr.mgh.harvard.edu (D.S. Manoach).

http://dx.doi.org/10.1016/j.nicl.2014.06.002

MRI (fMRI) activation of the anterior cingulate cortex (ACC). These error markers have been theorized to index error-based reinforcement learning (Holroyd and Coles, 2002), mismatch or conflict monitoring (Carter and van Veen, 2007; Falkenstein et al., 2000; Yeung et al., 2004), increased cognitive control (Kerns et al., 2004) and the emotional response to errors (Proudfit et al., 2013). Prior studies of OCD have demonstrated an exaggerated ERN (Carrasco et al., 2013; Endrass et al., 2008, 2010; Gehring et al., 2000; Johannes et al., 2001; but see Nieuwenhuis et al., 2005; Ruchsow et al., 2005; Xiao et al., 2011), increased rostral ACC (rACC) and/or dorsal ACC (dACC) activation following errors (Fitzgerald et al., 2005, 2010; Maltby et al., 2005; Stern et al., 2011; Ursu et al., 2003), and inappropriate error signaling on correct trials in some (Maltby et al., 2005; Ursu et al., 2003), but not all studies (Fitzgerald et al., 2005; Gehring et al., 2000). We expected to replicate prior findings that exaggerated error signaling correlates with symptom severity in OCD (Fitzgerald et al., 2005; Gehring et al., 2000; Ursu et al., 2003). This would support the theory that inappropriate and exaggerated error signaling leads to a pervasive sense of incompleteness and self-doubt and triggers compulsions to repeat behaviors (Maltby et al., 2005; Pitman, 1987).

Second, we investigated whether patients with OCD use errors to adjust future responses. To this end we examined post-error slowing (PES; Rabbitt, 1966), or the slowing of responses in trials that follow errors, and its neural correlates. Over trials, responses speed up until an error is committed (i.e., pre-error speeding; Gehring and Fencsik, 2001; Ridderinkhof et al., 2003) and following errors, responses slow down, presumably to reduce the probability of another error. (PES does not always lead to better performance, however, alternative accounts of its function exist (for review see, Danielmeier and Ullsperger, 2011) including that it reflects an orienting response to infrequent events (Notebaert et al., 2009).) These adjustments of reaction time (RT) are paralleled by changes in activity of the brain's default network (Agam et al., 2013). The default network, which is thought to mediate self-referential and affective processing, is typically deactivated during effortful cognitive performance, presumably reflecting reduced focus on the internal milieu (Buckner et al., 2008). During trials immediately preceding errors (Agam et al., 2013; Eichele et al., 2008; Li et al., 2007) and during error trials (Agam et al., 2013; Polli et al., 2005), there is a relative failure of this task-induced deactivation, suggesting that interference from internally directed thought culminates in an error. In trials that follow errors, task-induced deactivation is re-instated (Eichele et al., 2008), suggesting a shift in focus from the internal milieu back to the task-at-hand (Agam et al., 2013). Such dynamic modulations of attention and performance in response to outcomes are fundamental to adaptive, flexible behavior and we hypothesized that individuals with OCD would show abnormal post-error adjustments. We compared RT in correct trials immediately preceding an error and correct trials immediately following an error (i.e., PES), and the corresponding pattern of default network activation, as we have done in our prior work (Agam et al., 2011, 2013). Use of only pre-error and post-error correct trials maximizes sensitivity to changes in performance and activation based on error history because it minimizes contamination by global fluctuations in performance over time that affect comparisons that include all correct trials that follow a correct response (Dutilh et al., 2012). We expected that abnormal adjustments in the trial after an error in OCD would correlate with symptom severity.

We also examined error positivity or Pe (van Veen and Carter, 2002), an event-related potential occurring approximately 300–500 ms following an error (for review see, Overbeek et al., 2005). The Pe is less consistently observed than the ERN and is thought to index error awareness (Endrass et al., 2007; Nieuwenhuis et al., 2001; Wessel et al., 2011) and/or the subjective appraisal of errors (van Veen and Carter, 2002) and has been associated with PES (Nieuwenhuis et al., 2001).

Finally, we examined the microstructural integrity of the cingulum bundle using diffusion tensor imaging (DTI) measures of fractional anisotropy (FA). The cingulum bundle contains direct white matter connections between the ACC and the posterior cingulate cortex (PCC) (Schmahmann et al., 2007), and recent evidence suggests that these regions work together to mediate error processing (Agam et al., 2011). The rACC and PCC are also key anatomical components of the default network, whose activation corresponds with PES (Agam et al., 2013) and may mediate post-error adjustments. We investigated whether abnormal cingulate cortex function in OCD is accompanied by abnormal structural connectivity.

In summary, we expected OCD to be characterized by exaggerated and inappropriate error signaling and aberrant neural and behavioral adjustments following errors. Further, we expected that these abnormalities would predict symptom severity and have an anatomic correlate in the microstructural integrity of the cingulum bundle.

2. Methods

2.1. Participants

Sixty patients from the Obsessive–Compulsive and Related Disorders Program at Massachusetts General Hospital were enrolled. Twenty-seven met the following inclusion criteria and were referred for scanning: OCD based on a Structured Clinical Interview for DSM-IV (First et al., 1997); Yale–Brown Obsessive Compulsive Scale (Y-BOCS; Goodman et al., 1989a,b) total score >16; no co-morbid Axis I disorder with the exception of anxiety disorders and depression; and unmedicated or on stable medications for at least 8 weeks. Twenty-one of the 27 OCD patients referred for scanning completed the study. These participants had Y-BOCS scores of 11 ± 3 (mean ± SD) obsessions, 12 ± 3 compulsions, and 23 ± 5 total. Table S1 provides co-morbidity and medications.

Twenty healthy control participants, screened to exclude a personal history of mental illness (SCID — Non-patient Edition; First et al., 2002) and a family history of anxiety disorder, were recruited from the community by poster and website advertisements.

All participants were screened to exclude substance abuse or dependence within the preceding six months and any independent condition that might affect brain function. OCD patients were characterized with the Beck Depression Inventory-II (BDI-II, Beck, 1996) and Beck Anxiety Index (BAI; Beck et al., 1988; Table S1). The final groups of 21 OCD patients and 20 controls did not differ significantly in age, sex, years of education, handedness based on the modified Edinburgh Handedness Inventory (Oldfield, 1971; White and Ashton, 1976), or estimated verbal IQ based on the Wide Range Achievement Test-III Reading portion (Wilkinson, 1993) (Table 1). The study was approved by the Partners Human Research Committee and all participants gave written informed consent.

All participants were included in DTI analyses. To obtain reliable estimates of differences in activation, only participants with a minimum of ten usable error trials (Olvet and Hajcak, 2009; Pontifex et al., 2010)

Table 1
Means, standard deviations, and group comparisons of demographic data. The Phi value is the result of a Fisher's exact test. The z value is the result of a nonparametric Mann–Whitney U comparison.

Subject characteristics	Healthy controls (n = 20)	OCD (n = 21)	t	p
Age	33 ± 11	33 ± 11	0.07	.94
Sex	11M/9F	8M/13F	ϕ = .17	.35
Years of education	17 ± 2	16 ± 1	1.33	.19
Laterality score (handedness)[a]	65 ± 55	74 ± 34	0.62	.54
Estimated verbal IQ[b]	113 ± 6	110 ± 11	1.10	.28

[a] Laterality scores of −100 and +100 denote exclusive use of left or right hand, respectively.
[b] Two control participants and one OCD patient were not administered the WRAT-III because they were non-native English speakers.

were included in comparisons of error with correct trials (fMRI: n = 19 OCD, n = 15 controls; EEG: n = 19 OCD, n = 16 controls), and only participants with a minimum of ten usable pairs of correct pre- and post-error trials were included in fMRI analyses of post-error adjustments (n = 17 OCD, n = 14 controls).

2.2. Antisaccade paradigm

The antisaccade paradigm is described in Fig. 1. The task was programmed in MATLAB Psychtoolbox (Mathworks, Natick, MA) and consisted of three types of antisaccade trials: hard (40%), easy (50%), and fake-hard (10%). Hard trials introduced a distraction during the gap, a 3 dB luminance increase of the peripheral squares that mark the location of stimulus appearance. Fake-hard trials started with a cue indicating a hard trial, but were otherwise identical to easy trials (i.e., there was no luminance change). They were included as a control condition to allow us to examine the effects of a hard vs. easy cue on fMRI activation unconfounded by the change in luminance that characterizes hard trials. As this was not the goal of the present study, error and correct trials were combined across trial types for analysis.

Antisaccade trials were balanced for right and left stimuli. Randomly interleaved with the saccadic trials were fixation epochs lasting 2, 4, or 6 s, which provided a baseline and introduced "temporal jitter" to optimize the analysis of rapid presentation event-related fMRI data (Buckner et al., 1998; Burock and Dale, 2000; Miezin et al., 2000). The schedule of events was determined using a technique that optimizes the statistical efficiency of event-related designs (Dale, 1999). Each task run lasted 5 min 16 s and generated an average of 64 antisaccade trials and 20 fixation epochs.

Prior to scanning, participants practiced in a mock MRI scanner, were encouraged to respond as quickly and accurately as possible, and were told that in addition to the base rate of pay, they would receive 5¢ for each correct response. Participants performed six task runs during fMRI and eight runs during EEG. The ISCAN fMRI Remote Eye Tracking Laboratory (ISCAN, Burlington, MA) recorded eye position during fMRI using a 120 Hz video camera. During EEG, eye movements were monitored using two pairs of bipolar EOG electrodes, one vertical (above and below the left eye) and one horizontal. Horizontal EOG activity recorded during a brief calibration allowed an estimate of gaze position for scoring antisaccades (Endrass et al., 2005, 2007).

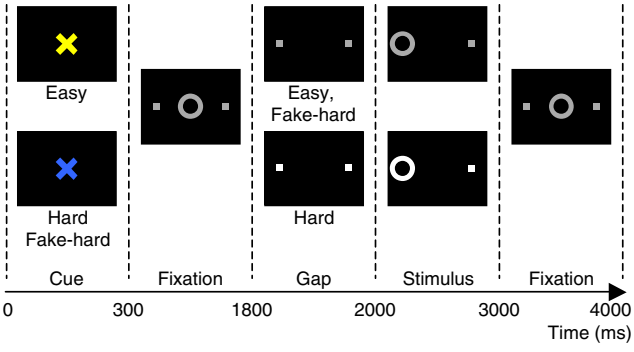

Fig. 1. Antisaccade paradigm. Schematic and timeline of the three conditions: easy, hard, and fake-hard. Each trial lasted 4 s and began with an instructional cue (300 ms), either a blue or yellow "X" that indicated whether the trial was hard or easy. The mapping of cue color to trial type was counterbalanced across participants. The cue was horizontally flanked by two white squares of 0.4° width that marked the potential locations of stimulus appearance, 10° left and right of center. The squares remained visible for the duration of each run. At 300 ms, the instructional cue was replaced by a white fixation ring of 1.3° diameter at the center of the screen. At 1800 ms, the fixation ring disappeared (200 ms gap). At 2000 ms, the fixation ring reappeared at one of the two stimulus locations, right or left with equal probability. This was the imperative stimulus to which the participant responded by making a saccade in the opposite direction. The ring remained in the peripheral location for 1000 ms and then returned to the center, where participants were instructed to return their gaze for 1000 ms before the start of the next trial. Fixation epochs were simply a continuation of this fixation display. Hard trials were distinguished by a 3 dB increase in luminance of the peripheral squares starting during the gap. Except for the hard cue, fake-hard trials were identical to easy trials.

Eye movement data were scored in MATLAB (Mathworks, Natick, MA) using a partially automated program. Saccades were identified as horizontal eye movements with velocities exceeding 47°/s. The onset of a saccade was defined as the point at which the velocity of the eye first exceeded 31°/s. Trials with initial saccades in the direction of the stimulus were scored as errors. Reaction time (RT) was defined as the onset time of the initial saccade relative to the appearance of the stimulus. Post-error slowing (PES) was defined as the RT difference between correct trials immediately following an error trial and correct trials immediately preceding an error trial. Self-correction latency was defined as the latency between the onset of the initial erroneous saccade and the onset of the corrective saccade. Error rates were logit-transformed before analysis to normalize their distribution. Group differences in error rates, rate of error self-correction, RT and PES were assessed using between-group t-tests. PES in each group was assessed using a one-sample t-test.

2.3. MRI acquisition

Images were acquired with a 3 T Siemens Trio whole body high-speed imaging device equipped for echo planar imaging (EPI) (Siemens Medical Systems, Erlangen, Germany) and a 12-channel head coil. From each participant we acquired a structural scan, six functional scans and a DTI scan.

A high-resolution structural scan was acquired in the sagittal plane using a 3D RF-spoiled magnetization prepared rapid gradient echo (MP-RAGE) sequence (TR/TE/flip = 2530 ms/3.39 ms/7°, FOV = 256 mm, 176 1.33 × 1 mm in-plane sagittal slices, 1.33 mm thickness). Functional images were collected using a gradient echo T2* weighted sequence (TR/TE/flip = 2000 ms/30 ms/90°, 32 contiguous horizontal slices parallel to the inter-commissural plane, voxel size: 3.1 × 3.1 × 3.7 mm, interleaved). The functional sequences included prospective acquisition correction (PACE) for head motion (Thesen et al., 2000). Single-shot echo planar imaging DTI was acquired using a twice refocused spin echo sequence with the following parameters: TR/TE = 7980/84 ms; b = 700 s/mm^2; 10 T2 images acquired with b = 0; 60 diffusion directions; 128 × 128 matrix; 2 × 2 mm in-plane resolution; 64 axial oblique (AC–PC) slices; 2 mm (0 mm gap) slice thickness; scan duration 9 min, 44 s.

2.4. fMRI data analysis

2.4.1. Surface-based projection

fMRI analyses were conducted on each participant's inflated cortical surfaces reconstructed from the MP-RAGE scan using FreeSurfer (http://surfer.nmr.mgh.harvard.edu) segmentation, surface reconstruction, and inflation algorithms (Dale et al., 1999; Fischl et al., 1999). Functional and structural scans were spatially normalized to a template brain consisting of the averaged cortical surface of an independent sample of 40 adults (Buckner Laboratory, Washington University, St. Louis, MO) using FreeSurfer's surface-based spherical coordinate system that employs a non-rigid alignment algorithm that explicitly aligns cortical folding patterns and is relatively robust to inter-individual differences in the gyral and sulcal anatomy of the cingulate cortex. Cortical activation was localized using automated surface-based parcellation software (Fischl et al., 2004).

To facilitate comparison with other studies, approximate Talairach coordinates were derived by mapping surface-based coordinates back to the original structural volume for each of the individuals whose brains were used to create the template brain, registering the volumes to the Montreal Neurological Institute (MNI305) atlas (Collins et al., 1994) and averaging the corresponding MNI305 coordinates. These coordinates were transformed to standard Talairach space using an

algorithm developed by Matthew Brett (http://imaging.mrc-cbu.cam.ac.uk/imaging/MniTalairach).

2.4.2. Functional data analysis

In addition to on-line motion correction (PACE), functional scans were retrospectively corrected for motion using AFNI (Cox and Jesmanowicz, 1999), intensity normalized, and smoothed using a 3D 8 mm FWHM Gaussian kernel. Functional images were aligned to the MP-RAGE scan for each participant. Residual head motion for each participant was calculated as the total displacement in millimeters in the x, y, and z directions and the total angular rotation in three directions (pitch, roll and yaw) from the initial head position for each run as determined by the AFNI motion correction algorithm. Displacement and rotation values were averaged for the six runs of the task and compared between groups.

Finite impulse response (FIR) estimates (Burock and Dale, 2000; Miezin et al., 2000) of the event-related hemodynamic responses were calculated for each trial type (i.e., pre-error and post-error, error and correct) for each participant. This involved using a linear model to provide unbiased estimates of the average signal intensity at each time point for each trial type without making a priori assumptions about the shape of the hemodynamic response. Estimates were computed at 12 time points with an interval of 2 s (corresponding to the TR) ranging from 4 s prior to the start of a trial to 18 s after the start. Temporal correlations in the noise were accounted for by prewhitening using a global estimate of the residual error autocorrelation function truncated at 30 s (Burock and Dale, 2000).

To test the hypothesis of exaggerated error signaling in OCD, we compared activation for correct and error trials at 6 s: the time point of maximum error-related activity in a prior antisaccade study (Polli et al., 2005). To test the hypothesis of impaired post-error adjustment in OCD, we compared activation during the preparatory period of post- and pre-error trials at 4 s: the time of peak preparatory ocular motor activity in prior studies (Manoach et al., 2007; Polli et al., 2005). Group comparisons used t-tests at each vertex. To examine correlations between activation and symptom severity in OCD, we regressed activation on Y-BOCS scores.

To correct for multiple comparisons, 10,000 Monte Carlo simulations of synthesized white Gaussian noise were run using the smoothing, resampling, and averaging parameters of the surface-based functional analysis to determine the likelihood that a cluster of a certain size would be found by chance for a given threshold ($p \leq .05$) on the cortical surface and to provide cluster-wise probability (CWP) values.

2.4.3. Region of interest (ROI) definitions

For error vs. correct comparisons the rACC and dACC were defined using automated surface-based parcellation software (Fischl et al., 2004) that delineated the cingulate cortex and divided it into rACC, dACC, and PCC (Desikan et al., 2006).

For analysis of post-error adjustments a default network ROI was defined using seed-based functional connectivity analysis of the functional data of all participants. A seed in the PCC was defined, based on prior studies (Andrews-Hanna et al., 2007; Van Dijk et al., 2010), as a 4 mm radius sphere centered at MNI coordinates $x = 0$, $y = -53$, $z = 26$. Pre-processing of the functional data of all participants involved: 1) registering the motion-corrected fMRI scans to the Montreal Neurological Institute (MNI152) atlas using FSL (FMRIB Software Library, www.fmrib.ox.ac.uk/fsl); 2) spatial smoothing using a Gaussian kernel of 6 mm full-width at half maximum; 3) temporal filtering (0.009 Hz to 0.08 Hz); and 4) removal of spurious or nonspecific sources of variance by regression of the following variables: (a) the six movement parameters computed by rigid body translation and rotation in preprocessing, (b) the mean whole brain signal, (c) the mean signal within the lateral ventricles, and (d) the mean signal within a deep white matter ROI. The first temporal derivatives of these regressors were included in the linear model to account for the time-shifted versions of spurious variance. Regression of each of these signals was computed simultaneously and the residual time course was retained for the correlation analysis. Functional connectivity maps were created by computing the Pearson correlation of the signal averaged across the voxels in the PCC seed region with that of every other voxel in the brain. Correlation maps for each individual were converted to a map of z-scores using Fisher's z transforms.

Determination of functional connectivity in the averaged group data was based on t-tests of the z-scores at each voxel. The default network was defined as vertices with positive connectivity that exceeded a Bonferroni corrected (for all gray matter voxels based on segmentation) threshold of $p \leq 3.3 * 10^{-7}$, which set the overall probability to .05 (Table S2). The functional connectivity analysis was conducted in the volume and the resulting statistical map was projected onto the cortical surfaces (Fig. S1).

2.5. EEG acquisition and analysis

EEG was acquired using a 70-channel electrode cap. Electrode impedances were brought below 20 kΩ at the start of each recording session. All signals were identically filtered to 0.1–200 Hz bandpass and digitized at 600 Hz. After excluding noisy EEG channels by visual inspection of the raw data, EEG data were re-referenced to the grand average. Each participant's continuous EEG data were low-pass filtered at 40 Hz. Trials with eye blinks were defined by a difference between the maximum and minimum voltage of 150 μV or greater at the vertical EOG channel and excluded from analysis.

EEG data, time-locked to saccadic onset, were baseline-corrected by subtracting the mean signal during the 100 ms preceding the saccade from the 500 ms that followed the saccade. Data for each of two trial types (all correct antisaccades and all errors) were averaged for each participant. Instead of using data from either FCz of Cz alone, the ERN was derived from the average signal across the following 10/20 locations: FC1, FCz, FC2, C1, Cz, C2, CP1, CPz, and CP2 for each participant to avoid participant exclusion for bad channels. On average, participants had 7/9 usable electrodes. Unusable data was seen in five control and nine OCD participants at Cz and in five control and two OCD participants at FCz. The peak ERN for the combined group of control and OCD participants was identified within the 200 ms following saccadic initiation as the point of maximal difference for the error vs. correct waveforms (which occurred at 140 ms). The peak ERN for each participant was identified as the point of maximal difference within 50 ms on either side of the group peak. The Pe was derived using the same set of electrodes as the ERN (Overbeek et al., 2005) and because a clear peak was absent in many participants (particularly those with OCD), Pe was defined as the mean difference in the error vs. correct waveforms between 300 and 500 ms following the initial saccade.

2.6. DTI analysis

Raw diffusion data were corrected for head motion and residual eddy current distortion by registering all images to the first acquired T2 ($b = 0$) image, using the FLIRT tool (Jenkinson and Smith, 2001) with a 12-df global affine transformation, available through the FSL. The diffusion tensor and FA volumes were reconstructed using the standard least-squares fit to the log diffusion signal (Basser et al., 1994). FA volumes were registered to the high-resolution structural (T1) volumes for each participant using the T2 ($b = 0$) volume as an intermediary. Inter-participant registration of individual FA maps to the Montreal Neurological Institute (MNI305) atlas was performed using each participant's T1 structural image, and the resulting transformation was applied to individual FA volumes. The MNI-normalized FA volumes were smoothed with a 3D Gaussian kernel with 6-mm full-width at half-maximum (FWHM).

We compared FA in OCD and control groups with t-tests at each voxel in the cingulum bundle identified using the Jülich Histological Atlas (Eickhoff et al., 2005). Multiple comparisons correction within the

cingulum bundle was based on Monte Carlo simulations of synthesized white Gaussian noise using the smoothing, resampling, and averaging parameters of the DTI analysis to set the overall threshold to $p \leq .05$.

3. Results

3.1. Antisaccade performance

Table 2 summarizes behavioral results. OCD patients made more errors than controls (trend in fMRI, significant in EEG). The groups did not differ significantly in the proportion of errors committed on hard trials, the proportion of self-corrected errors or the latency of correct responses. OCD patients showed a trend to have faster corrective saccades than controls during EEG. In the EEG data, controls showed significant PES, OCD patients showed a trend, and the groups did not differ significantly. Neither group showed significant PES in the fMRI data. Given the size of PES (13 ms on average for controls measured by EOG), the faster sampling rate of EOG (600 Hz) compared to the fMRI video camera (120 Hz) may have been necessary to detect PES. In OCD, neither error rate nor PES correlated with Y-BOCS scores.

3.2. Error markers

OCD and control groups did not differ in residual head motion during fMRI (displacement: control 1.9 ± 0.8 mm, OCD: 2.0 ± 0.5 mm, $t(37) = 0.28$, $p = .78$; rotation: control $0.8 \pm 0.5°$, OCD $0.7 \pm 0.35°$, $t(37) = 1.02$, $p = .31$). Both groups showed significant error-related dACC activation and did not differ significantly (Fig. 2A, Table 3A). Similarly, both groups showed a significant ERN (control: $t(15) = 7.73$, $p < 10^{-5}$; OCD: $t(18) = 6.10$, $p < 10^{-5}$) that did not significantly differ in peak amplitude (control: 3.59 ± 1.85 μV; OCD: 3.89 ± 2.77 μV; $t(33) = 0.43$, $p = .67$; Fig. 2B) or latency (control: 137 ± 29 ms; OCD: 126 ± 28 ms; $t(33) = 1.12$, $p = .27$). The ERN was derived using the average signal across nine electrodes. Considering the data from either Cz or FCz alone or their average, the ERN did not differ significantly between groups and was qualitatively similar to the results averaged over all nine electrodes. In the averaged group data, the ERN peaked ~140 ms, which is within the range of other ERN studies that measured the *onset* of movement with EMG or saccadic measurements (e.g., Gehring and Fencsik, 2001; Gehring et al., 1993; Nieuwenhuis et al., 2001), rather than its outcome (e.g., button presses), which results in shorter ERN latency (see Agam et al., 2011 for review; Carter and van Veen, 2007; Gehring et al., 2012). In both groups, the ERN was maximal at electrode CPz (Fig. S2). Finally, the Pe showed a trend to be reduced in OCD patients relative to control participants ($F(1,33) = 3.98$, $p = .06$; Fig. 2). There were no significant correlations of error-related activation in the ACC, ERN peak amplitude, or Pe with Y-BOCS scores in OCD.

3.3. Post-error adjustments

Control participants showed the expected pattern of default network activation: a failure of task-induced deactivation in the pre-error trial and a reinstatement of significant task-induced deactivation following an error (Fig. 3A, Table 3B). OCD participants showed an opposite pattern: significant task-induced deactivation in the pre-error trial and a relative failure of task-induced deactivation after the error. This pattern of post-error adjustment (post- vs. pre-error trials) significantly differed between groups in the left rACC and PCC nodes of the default network. OCD patients also showed significantly greater activation of the left PCC than controls in the post-error trial vs. fixation. Greater activation of the right rACC in post-error trials in OCD correlated with more severe compulsions and total Y-BOCS scores (Fig. 3B; Table 3B).

3.4. DTI

Relative to control participants, OCD patients showed increased FA in the cingulum bundle (Fig. 4). The peak of the group difference corresponded to the right rACC region in which post-error activation correlated with symptoms (MNI coordinates: $x = 6$, $y = 30$, $z = -4$; clusterwise probability (CWP) = 0.001). No other regions showed group differences that surpassed correction for multiple comparisons in the entire brain. FA in the cingulum bundle did not correlate with Y-BOCS scores, error-related dACC activation, ERN, or post-error adjustment.

3.5. Control analyses

3.5.1. Effects of EEG saccadic artifacts on the ERN

As in prior antisaccade studies (Endrass et al., 2005, 2007; Nieuwenhuis et al., 2001), the horizontal EOG for saccades to the left and right were almost identical in amplitude but of opposite polarity (Fig. S3A). Because there were an equal number of stimuli to the right and left and the proportion of errors to the right and left did not differ within individuals (control: $t(15) = 1.09$, $p = .29$; OCD: $t(18) = 0.51$, $p = .62$), the effects of the horizontal component of the eye movements are effectively eliminated in the averaged correct and error waveforms. The remaining vertical component of the saccadic artifact peaks at 19 ms and has the same polarity for left and right (Fig. 2B). It consists of a positive deflection that returns to baseline ~100 ms before

Table 2
Means, standard deviations, and group comparisons of task performance.

		Healthy controls	OCD	t	p
Error rate[a]	fMRI	12 ± 11%	14 ± 9%	1.67	.10
	EEG	13 ± 12%	16 ± 8%	2.10	.04
Percent of errors committed on hard trials[a]	fMRI	72 ± 16%	70 ± 15%	0.36	.72
	EEG	75 ± 17%	70 ± 13%	1.54	.13
Rate of error self-correction	fMRI[b]	99 ± 1%	98 ± 1%	0.57	.57
	EEG[c]	99 ± 0%	98 ± 1%	0.90	.37
Correct response latency[a]	fMRI	283 ± 11 ms	267 ± 10 ms	1.05	.30
	EEG	258 ± 10 ms	237 ± 11	1.35	.18
Self-correction latency	fMRI[b]	179 ± 9 ms	180 ± 8 ms	0.04	.97
	EEG[c]	194 ± 8 ms	174 ± 8 ms	1.79	.08
Post-error slowing	fMRI[d]	5 ± 19 ms	6 ± 27 ms	0.12	.91
(post-error − pre-error latency)	EEG[b]	13 ± 19*	6 ± 13 ms**	1.42	.17

[a] Based on 20 control and 21 OCD participants (i.e., the entire sample prior to exclusion based on the number of usable error trials).
[b] Based on 15 control and 19 OCD participants.
[c] Based on 18 control and 19 OCD participants.
[d] Based on 14 control and 17 OCD participants.
* Within-group paired comparison of post and pre-error latency: $t(14) = 2.67$, $p = .02$.
** Within-group paired comparison of post and pre-error latency: $t(18) = 1.85$, $p = .08$.

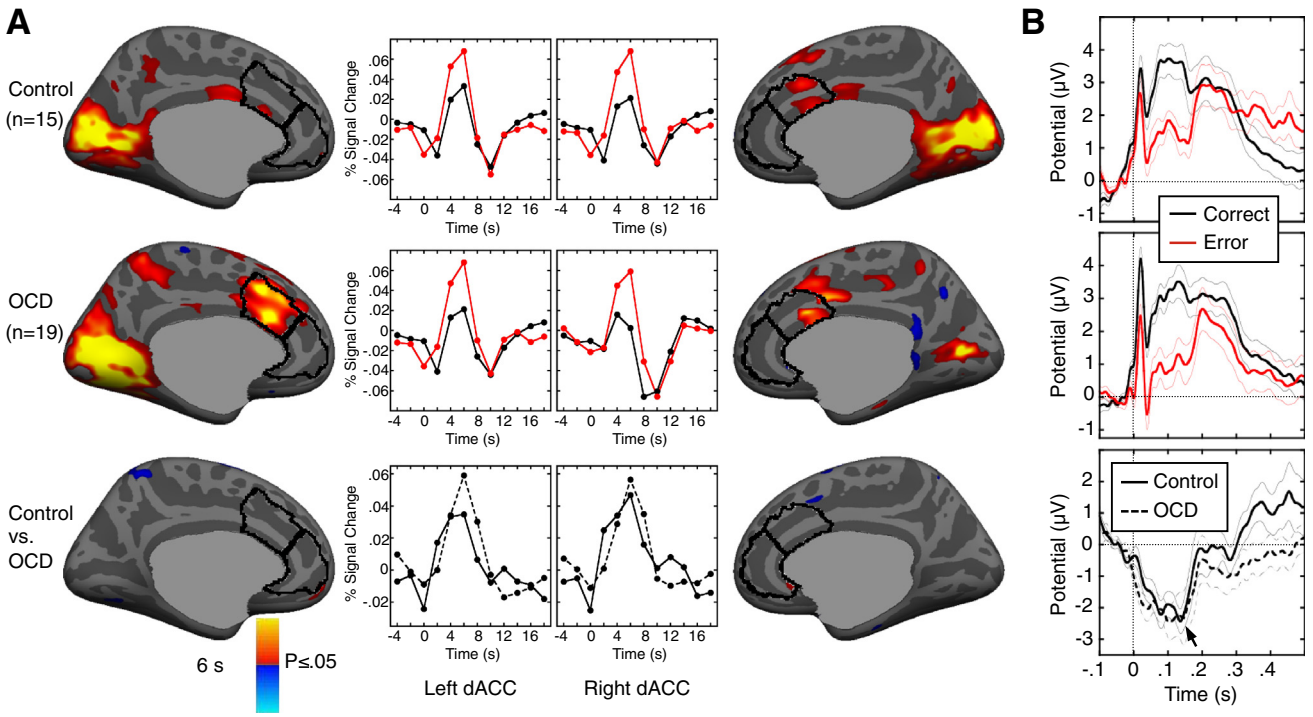

Fig. 2. Neural responses to error commission. A. Pseudocolor statistical maps of error-related fMRI activation at 6 s in the error vs. correct contrast are displayed on inflated medial cortical surfaces. The rACC and dACC ROIs are outlined in black. Gray masks cover subcortical regions in which activation is displaced in surface-based analyses. In the first two rows, warm colors indicate greater activation on error than correct trials. The third row shows the group comparison of error-related activation. The middle columns show hemodynamic response functions for each condition (correct: black; error: red) and for the error-correct difference for each group (Control: solid line; OCD: dashed line) for the left and right dACC ROIs. B. Plots in the first two rows show grand average EEG waveforms, with standard error lines, for correct (black) and error (red) trials, time-locked to the onset of the saccade (0 s), for control (first row) and OCD (second row) participants. The first peak after saccadic onset is eye movement artifact, which subtracts out of the difference waveform for error and correct trials, shown in the third row for each group. The arrow denotes the approximate time of peak ERN, which did not differ significantly by group.

the peak of the ERN and is mostly eliminated when the correct and error waveforms are subtracted to derive the ERN. It therefore does not contribute to the ERN. Nor does artifact from corrective saccades on error trials substantially affect the ERN. At the same EEG locations used to measure the ERN, we quantified the effect of the corrective saccade (Fig. S3B). The slope of the resulting signal, time-locked to saccadic onset, is smaller that that of the ERN and is similar for OCD and control groups. In addition, corrective saccades are jittered in time relative to the error, which reduces their effect. Finally, on average, corrective saccades are initiated later than the peak ERN (controls: 54 ± 33 ms; OCD: 34 ± 35 ms Fig. S3C).

3.5.2. Comparison of the correct EEG waveform in OCD vs. controls

A two-way ANOVA with factors trial type (correct, error) and group (control, OCD) on the average potentials between 90 and 190 ms after the response (i.e., the time window used for defining individual ERN peaks), using the same set of nine electrodes as the ERN analysis, showed the expected strong main effect of trial type ($F(1,33) = 22.05$, $p < 10^{-4}$), but no effect of group ($F(1,33) = 0.33$, $p = .57$) and no interaction of group with trial type ($F(1,33) = 0.20$, $p = .65$). Neither correct ($t(33) = 0.17$, $p = .87$) nor error ($t(33) = 0.76$, $p = .45$) waveforms differed between groups indicating that our non-replication of the finding of an exaggerated ERN in OCD (e.g., Gehring et al., 2000) was not due to an abnormally high amplitude correct waveform.

3.5.3. Effects of group differences in error rate on the ERN, dACC activation and neural indices of post-error adjustment

Error rates often inversely correlate with ERN and dACC activation (Holroyd and Coles, 2002; Polli et al., 2008; Santesso et al., 2006). Regression of activation (or ERN) on error rate with a group by error rate interaction showed that this was true in the present study for left and right dACC activation (left: $r(32) = -0.39$, $p = .02$; right: $r(32) = -0.47$; $p = .005$) and that there were no group differences in the slopes of these relations (p's ≥ .75). Error rate was not significantly correlated with the ERN ($r(33) = -0.10$, $p = .55$) and there was no group difference in slopes ($p = .71$). While OCD participants made more errors than controls, this difference was eliminated after participants were excluded from the functional analyses based on having made an insufficient number of errors (fMRI: control 15 ± 11%, OCD 14 ± 9%, $t(32) = 0.11$, $p = .91$; EEG: control 16 ± 11%, OCD 16 ± 8%, $t(33) = 0.79$, $p = .44$) and therefore does not account for the non-replication of findings of exaggerated error markers in OCD. A vertex-wise regression of post-error adjustment (contrast between post- vs. pre-error trials) on error rate with a group by error rate interaction term did not reveal significant relations within the default network ROI or the entire cortical surface and this did not differ by group.

3.5.4. Contributions of medication, depression, and anxiety to ERN and dACC activation

Seven OCD participants took various antidepressant medications, and one also took memantine (Table S1). Medicated patients did not significantly differ from medication-free patients in error-related dACC activation (left: $t(17) = 0.72$, $p = .48$; right: $t(17) = 1.03$, $p = .32$). Nor did post- vs. pre-error adjustments in default network activation differ significantly between medicated and unmedicated patients ($t(15) = 0.41$, $p = .69$; Fig. S4A). ERN amplitude was higher in medicated patients (Fig. S4B), but this did not reach significance ($t(17) = 1.68$, $p = .11$).

BDI-II and BAI symptom rating scale scores in OCD participants did not significantly correlate with either error-related dACC activation or error-related changes in the default network (i.e., there were no significant clusters). Nor did the ERN correlate with these ratings (BDI-II:

Table 3
Maxima and locations of significant clusters of activation. p-Values (−base − 10 log) are provided for the most significant vertex. A. Error-related fMRI activation in the ACC ROIs. Clusterwise probabilities (CWPs) are based on correction within the entire ACC. B. Default network activation in trials surrounding errors and correlations with Y-BOCS scores. CWPs are based on correction within the default network ROI. BA = Brodmann Area.

Cortical region	Size (mm^2)	Direction of effect	Talairach coordinates			BA	Max. p-value	CWP
			x	y	z			
A								
Error vs. correct								
Control (n = 15)								
Right dACC	272	Error > correct	13	17	31	32	2.45	.0001
Right dACC	179	Error > correct	5	15	22	24	2.11	.03
OCD (n = 19)								
Left dACC	1068	Error > correct	−5	23	22	32	4.84	.0001
Right dACC	969	Error > correct	6	19	28	32	4.16	.0001
Control vs. OCD								
None								
B								
Pre-error vs. fixation								
Control (n = 14)								
None								
OCD (n = 17)								
Left rACC	2365	Negative	−2	31	0	24	3.37	.0001
Left PCC	784	Negative	−7	−38	32	31	3.23	.0001
Left angular gyrus	551	Negative	−48	−57	41	39	2.17	.003
Right rACC	2661	Negative	4	31	3	24	3.54	.0001
Right PCC	1046	Negative	5	−31	32	31	3.26	.0001
Right middle temporal gyrus	703	Negative	60	−34	−5	21	3.11	.001
Right angular gyrus	578	Negative	46	−57	42	39	2.48	.005
Control vs. OCD								
None								
Post-error vs. fixation								
Control								
Left rACC	1331	Negative	−10	41	20	32	3.05	.0001
Left PCC	912	Negative	−15	−43	36	31	2.58	.0001
Left angular gyrus	518	Negative	−40	−64	39	39	3.27	.004
Right rACC	1757	Negative	10	46	12	9	3.75	.0001
Right PCC	577	Negative	6	−58	34	31	2.94	.005
OCD								
Right middle temporal gyrus	521	Negative	52	3	−25	38	2.50	.01
Control vs. OCD								
Left PCC	584	OCD > control	−16	−44	33	31	2.08	.002
OCD, relations with Y-BOCS scores								
Total								
Right rACC	475	r > 0	11	36	−5	32	2.74	.02
Obsessions								
Right rACC[a]	300	r > 0	10	35	−6	32	2.58	.16
Compulsions								
Right rACC	558	r > 0	14	39	−4	32	2.56	.008
Post-error vs. pre-error (adjustment)								
Control								
Left rACC	333	Negative	−11	37	−7	32	3.41	.008
Left rACC	289	Negative	−14	43	8	32	2.15	.02
OCD								
None								
Control vs. OCD								
Left rACC	950	OCD > control	−12	39	−7	32	2.78	.0001
Left PCC	358	OCD > control	−12	−51	28	31	2.25	.04

[a] Not significant, but shown in Fig. 3.

$r(17) = -0.27$, $p = .26$; BAI: $r(17) = -0.02$, $p = .94$). These findings suggest that neither medication nor the presence of anxious or depressive symptoms substantially affected our findings.

4. Discussion

OCD participants showed aberrant use of errors to adaptively adjust neural responses despite intact neural and behavioral indices of error detection (the ERN, error-related dACC activation and the rate of error self-correction). Control participants showed the expected pattern of adjustments based on prior work: a failure to deactivate the default network in pre-error and error trials (Agam et al., 2013; Eichele et al., 2008; Li et al., 2007; Polli et al., 2005) and a reinstatement of task-induced deactivation in post-error trials (Eichele et al., 2008). This pattern suggests that the error and pre-error trial are characterized by interference from self-referential thought and that the error prompts a shift in focus back to the task-at-hand in the subsequent trial. In contrast, OCD patients showed the opposite pattern, increased default network activation in the post-error compared to the pre-error trial and differed significantly from controls in this regard. This pattern suggests that rather than responding to errors by turning attention away from the internal milieu and back to the task-at-hand (Agam et al., 2013), the error prompted greater self-referential thought. This finding is consistent with previous reports that OCD participants show increased default network activation, specifically in the ventromedial prefrontal cortex, on error trials (Stern et al., 2011) and increased functional connectivity of the default network with the fronto-parietal attention network (Stern et al., 2012). These findings support the hypothesis that OCD is characterized

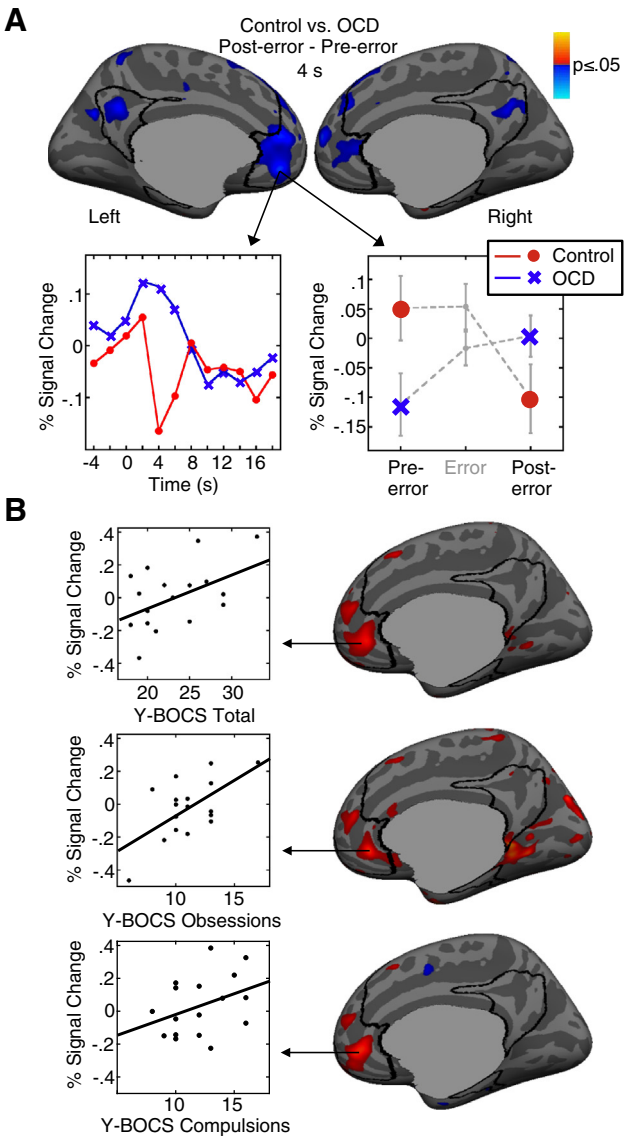

Fig. 3. Preparatory fMRI activation of the default network and its relation to symptom severity. Pseudocolor statistical maps of activation at 4 s are displayed on inflated medial cortical surfaces. The default network ROI is outlined in black. Gray masks cover subcortical regions in which activation is displaced in surface-based analyses. A: Preparatory fMRI activation in the group comparison of the post-error vs. pre-error contrast at 4 s. Blue indicates regions showing greater activation for OCD than controls in the post- vs. pre-error trial. The left graph shows the differences in hemodynamic responses for post-error minus pre-error trials for each group at the vertex with the maximum group difference in the post- vs. pre-error contrast. The right graph shows the means and standard errors for preparatory activation at this same vertex in the pre-error trial, error trial, and post-error trial. B: Relations between activation on post-error trials and Y-BOCS total, obsession, and compulsion scores. The scatter plots correspond to the maximum vertices in the correlation. In accord with recent practice in fMRI research, r-values from the maximum vertices are not reported since these are based on the present data and may therefore inflate the true correlation by adding the effect of random variability (e.g., Kriegeskorte et al., 2009; Vul and Pashler, 2012; Vul et al., 2009). The correlation with obsessions did not meet the cluster-wise probability threshold for significance.

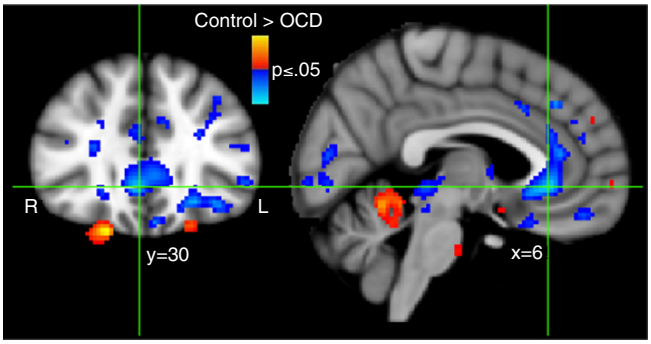

Fig. 4. DTI results. Pseudocolor statistical map of group differences in fractional anisotropy (FA) displayed on the MNI152 template brain. Red indicates higher FA in controls and blue indicates higher FA in OCD. Crosshairs denote the voxel of maximal significance.

by difficulty disengaging from evaluative processes when errors occur, which interferes with redirecting attention to the task-at-hand. The present finding of increased FA of rACC white matter in OCD, suggestive of increased default network structural connectivity, complements the findings of increased default network functional connectivity, although the target regions of the presumed increased rACC structural connectivity are unknown. Finally, the correlation of greater post-error activation of the rACC node of the default network with the severity of compulsions in OCD suggests that maladaptive neural responses to behavioral outcomes contribute to symptoms.

The severity of compulsions in OCD correlated with increased rACC activation in the post-error trial, but not with the post- vs. pre-error adjustment as predicted. Thus, this result should be considered preliminary. This correlation raises the possibility that more severely affected patients are simply more internally focused throughout the task and not just after an error. This is unlikely since default network activation in neither pre-error trials nor averaged across all correct trials correlated with symptoms, even without the cluster-wise correction for multiple comparisons. This relation may reflect that more symptomatic individuals dwell more on aversive and unexpected outcomes such as errors, or that aberrant neural responses to behavioral outcomes contribute to compulsive behavior. Alternatively, both aberrant adjustments to errors and compulsion severity may be influenced by a third factor, such as increased structural connectivity of the rACC as indexed by increased FA in the underlying white matter, which could either be a trait or reflect experience-dependent plasticity (Scholz et al., 2009). The cross-sectional correlative data of the present study does not allow us to resolve these important issues.

We also expected aberrant neural adjustments to errors to lead to abnormal behavioral adjustments and poorer performance. Neural adjustments did not correlate with PES or error rate. In the EEG latency data, controls showed significant PES, OCD patients showed a trend, and although the magnitude of PES in controls was more than twice that of OCD patients, the group difference did not reach significance. PES has been shown to be relatively small or absent on tasks with longer stimulus-to-response intervals as is the case in the present study (Danielmeier and Ullsperger, 2011; Jentzsch and Dudschig, 2009). Prior studies of OCD are inconsistent showing increased (Fitzgerald et al., 2005), intact (Endrass et al., 2008, 2010; Grundler et al., 2009; Hajcak and Simons, 2002; Santesso et al., 2006), and reduced (Liu et al., 2012) PES. With regard to antisaccade performance, considering the entire sample (i.e., before exclusion based on error-rate) OCD patients had a higher error rate than controls, consistent with some (Lennertz et al., 2012; Rosenberg et al., 1997; Tien et al., 1992) but not all (Jaafari et al., 2011; Spengler et al., 2006) studies and with other evidence of impaired response inhibition in OCD (Chamberlain et al., 2005; Menzies et al., 2007). Neural responses are likely to be more sensitive and specific indices of adjustments to errors than behavior.

Our findings of intact ERN and error-related dACC activation in OCD are discrepant with some prior work showing exaggerated error responses. Recent meta-analyses (Mathews et al., 2012; Moser et al., 2013) suggest that whether an exaggerated ERN is found depends on the task used and the type of symptoms present. Many prior studies used flanker tasks, and we cannot exclude the possibility that the discrepancies seen in the present study stem from the different movement modality or task requirements of antisaccades or that in both groups

virtually all errors were self-corrected. Reviews of the literature (Agam et al., 2011; Holroyd and Coles, 2002), however, indicate that the ERN and dACC activation are 'generic' indices of error processing that are present for errors in a range of contexts including errors committed with the feet (Holroyd et al., 1998), eyes, and hands in a variety of tasks. A prior study that compared ERNs generated by button presses and saccades found them to be similar in morphology, amplitude and scalp topography (Van 't Ent and Apkarian, 1999). In addition, in our prior antisaccade study, the ERN was compatible with those described in the literature with regard to scalp distribution, latency, and morphology (Agam et al., 2011). Thus, it is unlikely that antisaccades produce a fundamentally different ERN than other tasks used to study error processing. The present findings are consistent with the meta-analyses in suggesting that findings of exaggerated error markers in OCD may be task-dependent (Mathews et al., 2012; Moser et al., 2013). A caveat to this explanation of the discrepancies in our finding of a normal ERN is that in the meta-analysis of Matthews and colleagues, increased ERNs in OCD were seen for response conflict tasks, of which the antisaccade is an example, and, consistent with recent study (Riesel et al., 2014), are also seen across all symptom dimensions, except hoarding, which was not present in our sample.

A related concern is that the discrepancies may arise as a function of a deficit in volitional saccade generation in OCD. OCD patients and their syndromally-unaffected first-degree relatives have been shown to have longer latencies of volitional saccades (Kloft et al., 2013). In the present study, the latency to generate correct volitional antisaccades was actually non-significantly shorter for OCD than control participants suggesting intact generation of volitional saccades, despite the deficit in response inhibition (i.e., increased antisaccade error rate in the OCD sample prior to exclusion). Given that the latency for correct antisaccades and the neural markers of antisaccade errors were intact in OCD, it is unlikely that a deficit in generating volitional saccades accounts for our findings of intact ERN and error-related dACC activation in the context of a specific impairment in post-error neural adjustments.

Another potential source of inconsistency with the literature is that the ERN is variably defined based solely on error trials or on the difference between error and correct trials. If the waveform for correct trials is also more negative, as is sometimes seen in OCD (Endrass et al., 2008, 2010; Hajcak and Simons, 2002), difference waveforms are less likely to differentiate between groups. This was not the case in the present study since neither the correct nor the error waveforms differed in OCD. In the present study, we derived the ERN using the average signal across nine electrodes instead of using data from either FCz or Cz alone to avoid excluding participants based on bad channels. While we cannot exclude the possibility that missing data from either FCz or Cz in some participants affected our results, when the data from either Cz or FCz was considered alone or when their average was considered, the ERN did not differ significantly between groups and was qualitatively similar to the results from the data averaged over nine electrodes.

Methodological differences may have also contributed to the apparent discrepancy with prior findings of enhanced error-related ACC activation in OCD (Fitzgerald et al., 2005, 2010; Maltby et al., 2005; Stern et al., 2011; Ursu et al., 2003). Prior studies used analysis techniques that assume a shape to the hemodynamic response. A single assumed model is unlikely to be valid across all brain regions and stimulus types (Duann et al., 2002) and inaccurate models may misattribute activation to adjacent events (Manoach et al., 2003). For this reason, it is possible that increased ACC activation on error trials in prior studies reflects greater activation of the default network prior to error commission (Polli et al., 2005) rather than an exaggerated response to the error. In the present study, the relatively long cue-to-target interval of each trial and the use of FIR models, which make no a priori assumptions about the shape of the hemodynamic response, allow more accurate modeling of preparatory vs. error-related activation.

Other potential sources of discrepant findings include medication use in the OCD patients and sample size. In the present study, the subset of medicated OCD patients did not differ in dACC activation, but showed a non-significantly higher ERN, as was also seen in an earlier study that showed a normal ERN in OCD (Nieuwenhuis et al., 2005). Medications are unlikely to account for previous findings of exaggerated ERNs in OCD, however, since this has been reported in OCD patients regardless of medication use (Endrass et al., 2008; Stern et al., 2010) and in syndromally-unaffected first-degree relatives of OCD patients (Riesel et al., 2011). Nor is the non-replication likely to reflect a lack of power due to the relatively small sample size. The between-group effect sizes of the present study are so small (0.24 in the left dACC, 0.10 in the right dACC, and 0.09 for the ERN) that samples of well over 100 participants per group would be required to detect group differences with 80% power.

The relatively small sample size may have limited our power to evaluate the Pe, which is less well-characterized than the ERN and less consistently observed. The Pe showed a trend to be reduced in the present study of OCD, but not in prior work (Endrass et al., 2008, 2010; Ruchsow et al., 2005). Unlike the ERN, which is present regardless of whether errors are perceived, the Pe is present only for perceived errors and is thought to index error awareness (Endrass et al., 2007; Nieuwenhuis et al., 2001). While the literature lacks a clear consensus about its function (Overbeek et al., 2005), the Pe has also been associated with short-term performance adjustments such as PES (Nieuwenhuis et al., 2001). Given that in the present study the Pe reduction was not expected, did not reach statistical significance and did not correlate with PES, we are reluctant to speculate about how an abnormal Pe in OCD may relate to our main findings of aberrant neural adjustments to errors in the default network.

Finally, we expected to replicate correlations of increased error signaling with symptom severity in OCD (Fitzgerald et al., 2005; Gehring et al., 2000; Ursu et al., 2003). Neither ERN amplitude nor error-related dACC activation correlated with symptoms. These null findings are consistent with a prior study that reported no relations of ERN with symptom severity in OCD (Riesel et al., 2011). This study also found an increased ERN in syndromally-unaffected first-degree relatives leading the authors to suggest that overactive error monitoring is an endophenotype of OCD that is independent of the presence of clinical symptoms. In the present study, we instead found that increased rACC activation in trials that followed errors correlated with the severity of compulsions. As this is the first report of abnormal post-error neural adjustments, there is no evidence bearing on whether this represents a state or trait marker.

In summary, the present findings demonstrate aberrant neural adjustments to errors in OCD. This suggests an impairment in adaptively and dynamically responding to outcomes. Moreover, greater default network activation following an error correlated with the severity of compulsions. The rACC locus of the aberrant adjustment and relations with symptoms suggests difficulty suppressing emotional evaluative responses to aversive and unexpected outcomes such as errors. This may preclude more adaptive responses that would redirect attention to the task-at-hand and minimize the probability of error recurrence. Increased FA in rACC white matter suggests increased structural connectivity of this paralimbic default network region as an anatomic correlate of abnormal adjustment.

Supplementary data to this article can be found online at http://dx.doi.org/10.1016/j.nicl.2014.06.002.

Acknowledgments

The authors are grateful to Dr. Mark Vangel for statistical consultation.

Funding

The funding agencies, the David Judah Foundation (JLG, DSM) and the National Institute of Mental Health (F32 MH088081 (YA); R01MH67720 (DSM)), played no role in the design or conduct of the

study including data collection, management, analysis, and interpretation or in the preparation, review, or approval of the manuscript.

Financial disclosures

Dr. Wilhelm receives research funding from the National Institutes of Health (R01MH091078); royalties from Oxford University Press, New Harbinger Publications, and Guilford Publications; and support in the form of free medication and matching placebo from Forest Laboratories for a clinical trial funded by the National Institutes of Health; and has received speaking honoraria from various academic institutions. The other authors have no conflicts of interest to disclose.

References

Agam, Y., Hamalainen, M.S., Lee, A.K., Dyckman, K.A., Friedman, J.S., Isom, M., Makris, N., Manoach, D.S., 2011. Multimodal neuroimaging dissociates hemodynamic and electrophysiological correlates of error processing. Proc. Natl. Acad. Sci. U. S. A. 108, 17556–17561.

Agam, Y., Carey, C., Barton, J.J., Dyckman, K.A., Lee, A.K., Vangel, M., Manoach, D.S., 2013. Network dynamics underlying speed–accuracy trade-offs in response to errors. PLoS ONE 8, e73692.

Andrews-Hanna, J.R., Snyder, A.Z., Vincent, J.L., Lustig, C., Head, D., Raichle, M.E., Buckner, R.L., 2007. Disruption of large-scale brain systems in advanced aging. Neuron 56, 924–935.

Basser, P.J., Mattiello, J., LeBihan, D., 1994. MR diffusion tensor spectroscopy and imaging. Biophys. J. 66, 259–267.

Beck, A.T., 1996. BDI-II, Beck Depression Inventory: Manual. The Psychological Corporation, San Antonio, TX,.

Beck, A.T., Epstein, N., Brown, G., Steer, R.A., 1988. An inventory for measuring clinical anxiety: psychometric properties. J. Consult. Clin. Psychol. 56, 893–897.

Belopolsky, A.V., Kramer, A.F., 2006. Error-processing of oculomotor capture. Brain Res. 1081, 171–178.

Buckner, R.L., Goodman, J., Burock, M., Rotte, M., Koutstaal, W., Schacter, D., Rosen, B., Dale, A.M., 1998. Functional–anatomic correlates of object priming in humans revealed by rapid presentation event-related fMRI. Neuron 20, 285–296.

Buckner, R.L., Andrews-Hanna, J.R., Schacter, D.L., 2008. The brain's default network: anatomy, function, and relevance to disease. Ann. N. Y. Acad. Sci. 1124, 1–38.

Burock, M.A., Dale, A.M., 2000. Estimation and detection of event-related fMRI signals with temporally correlated noise: a statistically efficient and unbiased approach. Hum. Brain Mapp. 11, 249–260.

Carrasco, M., Harbin, S.M., Nienhuis, J.K., Fitzgerald, K.D., Gehring, W.J., Hanna, G.L., 2013. Increased error-related brain activity in youth with obsessive–compulsive disorder and unaffected siblings. Depress. Anxiety 30, 39–46.

Carter, C.S., van Veen, V., 2007. Anterior cingulate cortex and conflict detection: an update of theory and data. Cogn. Affect. Behav. Neurosci. 7, 367–379.

Chamberlain, S.R., Blackwell, A.D., Fineberg, N.A., Robbins, T.W., Sahakian, B.J., 2005. The neuropsychology of obsessive compulsive disorder: the importance of failures in cognitive and behavioural inhibition as candidate endophenotypic markers. Neurosci. Biobehav. Rev. 29, 399–419.

Collins, D.L., Neelin, P., Peters, T.M., Evans, A.C., 1994. Automatic 3D intersubject registration of MR volumetric data in standardized Talairach space. J. Comput. Assist. Tomogr. 18, 192–205.

Cox, R.W., Jesmanowicz, A., 1999. Real-time 3D image registration for functional MRI. Magn. Reson. Med. 42, 1014–1018.

Dale, A.M., 1999. Optimal experimental design for event-related fMRI. Hum. Brain Mapp. 8, 109–140.

Dale, A.M., Fischl, B., Sereno, M.I., 1999. Cortical surface-based analysis. I. Segmentation and surface reconstruction. Neuroimage 9, 179–194.

Danielmeier, C., Ullsperger, M., 2011. Post-error adjustments. Front. Psychol. 2, 233.

Desikan, R.S., Segonne, F., Fischl, B., Quinn, B.T., Dickerson, B.C., Blacker, D., Buckner, R.L., Dale, A.M., Maguire, R.P., Hyman, B.T., Albert, M.S., Killiany, R.J., 2006. An automated labeling system for subdividing the human cerebral cortex on MRI scans into gyral based regions of interest. Neuroimage 31, 968–980.

Duann, J.R., Jung, T.P., Kuo, W.J., Yeh, T.C., Makeig, S., Hsieh, J.C., Sejnowski, T.J., 2002. Single-trial variability in event-related BOLD signals. Neuroimage 15, 823–835.

Dutilh, G., van Ravenzwaaij, D., Nieuwenhuis, S., van der Maas, H.L.J., Forstmann, B.U., Wagenmakers, E.-J., 2012. How to measure post-error slowing: a confound and a simple solution. J. Math. Psychol. 56, 208–216.

Eichele, T., Debener, S., Calhoun, V.D., Specht, K., Engel, A.K., Hugdahl, K., von Cramon, D.Y., Ullsperger, M., 2008. Prediction of human errors by maladaptive changes in event-related brain networks. Proc. Natl. Acad. Sci. U. S. A. 105, 6173–6178.

Eickhoff, S.B., Stephan, K.E., Mohlberg, H., Grefkes, C., Fink, G.R., Amunts, K., Zilles, K., 2005. A new SPM toolbox for combining probabilistic cytoarchitectonic maps and functional imaging data. Neuroimage 25, 1325–1335.

Endrass, T., Franke, C., Kathmann, N., 2005. Error awareness in a saccade countermanding task. J. Psychophysiol. 19, 275–280.

Endrass, T., Reuter, B., Kathmann, N., 2007. ERP correlates of conscious error recognition: aware and unaware errors in an antisaccade task. Eur. J. Neurosci. 26, 1714–1720.

Endrass, T., Klawohn, J., Schuster, F., Kathmann, N., 2008. Overactive performance monitoring in obsessive–compulsive disorder: ERP evidence from correct and erroneous reactions. Neuropsychologia 46, 1877–1887.

Endrass, T., Schuermann, B., Kaufmann, C., Spielberg, R., Kniesche, R., Kathmann, N., 2010. Performance monitoring and error significance in patients with obsessive–compulsive disorder. Biol. Psychol. 84, 257–263.

Falkenstein, M., Hoormann, J., Christ, S., Hohnsbein, J., 2000. ERP components on reaction errors and their functional significance: a tutorial. Biol. Psychol. 51, 87–107.

First, M.B., Spitzer, R.L., Gibbon, M., Williams, J.B.W., 1997. Structured Clinical Interview for DSM-IV Axis I Disorders, Research Version, Patient Edition with Psychotic Screen (SCID-I/P W/PSY SCREEN). Biometrics Research, New York State Psychiatric Institute, New York,.

First, M.B., Spitzer, R.L., Gibbon, M., Williams, J.B.W., 2002. Structured Clinical Interview for DSM-IV-TR Axis I Disorders, Research Version, Nonpatient Edition. Biometrics Research, New York State Psychiatric Institute, New York,.

Fischl, B., Sereno, M.I., Dale, A.M., 1999. Cortical surface-based analysis. II: inflation, flattening, and a surface-based coordinate system. Neuroimage 9, 195–207.

Fischl, B., van der Kouwe, A., Destrieux, C., Halgren, E., Segonne, F., Salat, D.H., Busa, E., Seidman, L.J., Goldstein, J., Kennedy, D., Caviness, V., Makris, N., Rosen, B., Dale, A.M., 2004. Automatically parcellating the human cerebral cortex. Cereb. Cortex 14, 11–22.

Fitzgerald, K.D., Welsh, R.C., Gehring, W.J., Abelson, J.L., Himle, J.A., Liberzon, I., Taylor, S.F., 2005. Error-related hyperactivity of the anterior cingulate cortex in obsessive–compulsive disorder. Biol. Psychiatry 57, 287–294.

Fitzgerald, K.D., Perkins, S.C., Angstadt, M., Johnson, T., Stern, E.R., Welsh, R.C., Taylor, S.F., 2010. The development of performance-monitoring function in the posterior medial frontal cortex. Neuroimage 49, 3463–3473.

Gehring, W.J., Fencsik, D.E., 2001. Functions of the medial frontal cortex in the processing of conflict and errors. J. Neurosci. 21, 9430–9437.

Gehring, W.J., Goss, B., Coles, M.G., Meyer, D.E., Donchin, E., 1993. A neural system for error detection and compensation. Psychol. Sci. 4, 385–390.

Gehring, W.J., Himle, J., Nisenson, L.G., 2000. Action-monitoring dysfunction in obsessive–compulsive disorder. Psychol. Sci. 11, 1–6.

Gehring, W.J., Liu, Y., Orr, J.M., Carp, J., 2012. The error-related negativity (ERN/Ne). In: Luck, S.J., Kappenman, E. (Eds.), Oxford Handbook of Event-related Potential Components. Oxford University Press, NY, pp. 231–291.

Goodman, W.K., Price, L.H., Rasmussen, S.A., Mazure, C., Delgado, P., Heninger, G.R., Charney, D.S., 1989a. The Yale–Brown Obsessive Compulsive Scale. II. Validity. Arch. Gen. Psychiatry 46, 1012–1016.

Goodman, W.K., Price, L.H., Rasmussen, S.A., Mazure, C., Fleischmann, R.L., Hill, C.L., Heninger, G.R., Charney, D.S., 1989b. The Yale–Brown Obsessive Compulsive Scale. I. Development, use, and reliability. Arch. Gen. Psychiatry 46, 1006–1011.

Grundler, T.O., Cavanagh, J.F., Figueroa, C.M., Frank, M.J., Allen, J.J., 2009. Task-related dissociation in ERN amplitude as a function of obsessive–compulsive symptoms. Neuropsychologia 47, 1978–1987.

Hajcak, G., Simons, R.F., 2002. Error-related brain activity in obsessive–compulsive undergraduates. Psychiatry Res. 110, 63–72.

Holroyd, C.B., Coles, M.G., 2002. The neural basis of human error processing: reinforcement learning, dopamine, and the error-related negativity. Psychol. Rev. 109, 679–709.

Holroyd, C.B., Dien, J., Coles, M.G., 1998. Error-related scalp potentials elicited by hand and foot movements: evidence for an output-independent error-processing system in humans. Neurosci. Lett. 242, 65–68.

Jaafari, N., Rigalleau, F., Rachid, F., Delamillieure, P., Millet, B., Olie, J.P., Gil, R., Rotge, J.Y., Vibert, N., 2011. A critical review of the contribution of eye movement recordings to the neuropsychology of obsessive compulsive disorder. Acta Psychiatr. Scand. 124, 87–101.

Jenkinson, M., Smith, S., 2001. A global optimisation method for robust affine registration of brain images. Med. Image Anal. 5, 143–156.

Jentzsch, I., Dudschig, C., 2009. Why do we slow down after an error? Mechanisms underlying the effects of posterior slowing. Q. J. Exp. Psychol. 62, 209–218.

Johannes, S., Wieringa, B.M., Nager, W., Rada, D., Dengler, R., Emrich, H.M., Munte, T.F., Dietrich, D.E., 2001. Discrepant target detection and action monitoring in obsessive–compulsive disorder. Psychiatry Res. 108, 101–110.

Kerns, J.G., Cohen, J.D., MacDonald III, A.W., Cho, R.Y., Stenger, V.A., Carter, C.S., 2004. Anterior cingulate conflict monitoring and adjustments in control. Science 303, 1023–1026.

Klein, T.A., Endrass, T., Kathmann, N., Neumann, J., von Cramon, D.Y., Ullsperger, M., 2007. Neural correlates of error awareness. Neuroimage 34, 1774–1781.

Kloft, L., Reuter, B., Riesel, A., Kathmann, N., 2013. Impaired volitional saccade control: first evidence for a new candidate endophenotype in obsessive–compulsive disorder. Eur. Arch. Psychiatry Clin. Neurosci. 263, 215–222.

Kriegeskorte, N., Simmons, W.K., Bellgowan, P.S., Baker, C.I., 2009. Circular analysis in systems neuroscience: the dangers of double dipping. Nat. Neurosci. 12, 535–540.

Lennertz, L., Rampacher, F., Vogeley, A., Schulze-Rauschenbach, S., Pukrop, R., Ruhrmann, S., Klosterkotter, J., Maier, W., Falkai, P., Wagner, M., 2012. Antisaccade performance in patients with obsessive–compulsive disorder and unaffected relatives: further evidence for impaired response inhibition as a candidate endophenotype. Eur. Arch. Psychiatry Clin. Neurosci. 262, 625–634.

Li, C.S., Yan, P., Bergquist, K.L., Sinha, R., 2007. Greater activation of the "default" brain regions predicts stop signal errors. Neuroimage 38, 640–648.

Liu, Y., Gehring, W.J., Weissman, D.H., Taylor, S.F., Fitzgerald, K.D., 2012. Trial-by-trial adjustments of cognitive control following errors and response conflict are altered in pediatric obsessive compulsive disorder. Front. Psychiatry 3, 41.

Maltby, N., Tolin, D.F., Worhunsky, P., O'Keefe, T.M., Kiehl, K.A., 2005. Dysfunctional action monitoring hyperactivates frontal–striatal circuits in obsessive–compulsive disorder: an event-related fMRI study. Neuroimage 24, 495–503.

Manoach, D.S., Greve, D.N., Lindgren, K.A., Dale, A.M., 2003. Identifying regional activity associated with temporally separated components of working memory using event-related functional MRI. Neuroimage 20, 1670–1684.
Manoach, D.S., Thakkar, K.N., Cain, M.S., Polli, F.E., Edelman, J.A., Fischl, B., Barton, J.J., 2007. Neural activity is modulated by trial history: a functional magnetic resonance imaging study of the effects of a previous antisaccade. J. Neurosci. 27, 1791–1798.
Mathews, C.A., Perez, V.B., Delucchi, K.L., Mathalon, D.H., 2012. Error-related negativity in individuals with obsessive–compulsive symptoms: toward an understanding of hoarding behaviors. Biol. Psychol. 89, 487–494.
Menzies, L., Achard, S., Chamberlain, S.R., Fineberg, N., Chen, C.H., Del Campo, N., Sahakian, B.J., Robbins, T.W., Bullmore, E., 2007. Neurocognitive endophenotypes of obsessive–compulsive disorder. Brain 130, 3223–3236.
Miezin, F.M., Maccotta, L., Ollinger, J.M., Petersen, S.E., Buckner, R.L., 2000. Characterizing the hemodynamic response: effects of presentation rate, sampling procedure, and the possibility of ordering brain activity based on relative timing. Neuroimage 11, 735–759.
Moser, J.S., Moran, T.P., Schroder, H.S., Donnellan, M.B., Yeung, N., 2013. On the relationship between anxiety and error monitoring: a meta-analysis and conceptual framework. Front. Hum. Neurosci. 7, 466.
Nieuwenhuis, S., Ridderinkhof, K.R., Blom, J., Band, G.P., Kok, A., 2001. Error-related brain potentials are differentially related to awareness of response errors: evidence from an antisaccade task. Psychophysiology 38, 752–760.
Nieuwenhuis, S., Nielen, M.M., Mol, N., Hajcak, G., Veltman, D.J., 2005. Performance monitoring in obsessive–compulsive disorder. Psychiatry Res. 134, 111–122.
Notebaert, W., Houtman, F., Opstal, F.V., Gevers, W., Fias, W., Verguts, T., 2009. Post-error slowing: an orienting account. Cognition 111, 275–279.
Oldfield, R.C., 1971. The assessment and analysis of handedness: the Edinburgh inventory. Neuropsychologia 9, 97–113.
Olvet, D.M., Hajcak, G., 2009. The stability of error-related brain activity with increasing trials. Psychophysiology 46, 957–961.
Overbeek, T.J.M., Nieuwenhuis, S., Ridderinkhof, K.R., 2005. Dissociable components of error processing. J. Psychophysiol. 19, 319–329.
Pitman, R.K., 1987. A cybernetic model of obsessive–compulsive psychopathology. Compr. Psychiatry 28, 334–343.
Polli, F.E., Barton, J.J., Cain, M.S., Thakkar, K.N., Rauch, S.L., Manoach, D.S., 2005. Rostral and dorsal anterior cingulate cortex make dissociable contributions during antisaccade error commission. Proc. Natl. Acad. Sci. U. S. A. 102, 15700–15705.
Polli, F.E., Barton, J.J., Thakkar, K.N., Greve, D.N., Goff, D.C., Rauch, S.L., Manoach, D.S., 2008. Reduced error-related activation in two anterior cingulate circuits is related to impaired performance in schizophrenia. Brain 131, 971–986.
Pontifex, M.B., Scudder, M.R., Brown, M.L., O'Leary, K.C., Wu, C.T., Themanson, J.R., Hillman, C.H., 2010. On the number of trials necessary for stabilization of error-related brain activity across the life span. Psychophysiology 47, 767–773.
Proudfit, G.H., Inzlicht, M., Mennin, D.S., 2013. Anxiety and error monitoring: the importance of motivation and emotion. Front. Hum. Neurosci. 7, 636.
Rabbitt, P.M., 1966. Errors and error correction in choice–response tasks. J. Exp. Psychol. 71, 264–272.
Ridderinkhof, K.R., Nieuwenhuis, S., Bashore, T.R., 2003. Errors are foreshadowed in brain potentials associated with action monitoring in cingulate cortex in humans. Neurosci. Lett. 348, 1–4.
Riesel, A., Endrass, T., Kaufmann, C., Kathmann, N., 2011. Overactive error-related brain activity as a candidate endophenotype for obsessive–compulsive disorder: evidence from unaffected first-degree relatives. Am. J. Psychiatry 168, 317–324.
Riesel, A., Kathmann, N., Endrass, T., 2014. Overactive performance monitoring in obsessive–compulsive disorder is independent of symptom expression. Eur. Arch. Psychiatry Clin. Neurosci.
Rosenberg, D.R., Averbach, D.H., O'Hearn, K.M., Seymour, A.B., Birmaher, B., Sweeney, J.A., 1997. Oculomotor response inhibition abnormalities in pediatric obsessive–compulsive disorder. Arch. Gen. Psychiatry 54, 831–838.
Ruchsow, M., Gron, G., Reuter, M., Spitzer, M., Hermle, L., Kiefer, M., 2005. Error-related brain activity in patients with obsessive–compulsive disorder and in healthy controls. J. Psychophysiol. 19, 298–304.
Santesso, D.L., Segalowitz, S.J., Schmidt, L.A., 2006. Error-related electrocortical responses are enhanced in children with obsessive–compulsive behaviors. Dev. Neuropsychol. 29, 431–445.
Schmahmann, J.D., Pandya, D.N., Wang, R., Dai, G., D'Arceuil, H.E., de Crespigny, A.J., Wedeen, V.J., 2007. Association fibre pathways of the brain: parallel observations from diffusion spectrum imaging and autoradiography. Brain 130, 630–653.
Scholz, J., Klein, M.C., Behrens, T.E., Johansen-Berg, H., 2009. Training induces changes in white-matter architecture. Nat. Neurosci. 12, 1370–1371.
Spengler, D., Trillenberg, P., Sprenger, A., Nagel, M., Kordon, A., Junghanns, K., Heide, W., Arolt, V., Hohagen, F., Lencer, R., 2006. Evidence from increased anticipation of predictive saccades for a dysfunction of fronto-striatal circuits in obsessive–compulsive disorder. Psychiatry Res. 143, 77–88.
Stern, E.R., Liu, Y., Gehring, W.J., Lister, J.J., Yin, G., Zhang, J., Fitzgerald, K.D., Himle, J.A., Abelson, J.L., Taylor, S.F., 2010. Chronic medication does not affect hyperactive error responses in obsessive–compulsive disorder. Psychophysiology 47, 913–920.
Stern, E.R., Welsh, R.C., Fitzgerald, K.D., Gehring, W.J., Lister, J.J., Himle, J.A., Abelson, J.L., Taylor, S.F., 2011. Hyperactive error responses and altered connectivity in ventromedial and frontoinsular cortices in obsessive–compulsive disorder. Biol. Psychiatry 69, 583–591.
Stern, E.R., Fitzgerald, K.D., Welsh, R.C., Abelson, J.L., Taylor, S.F., 2012. Resting-state functional connectivity between fronto-parietal and default mode networks in obsessive–compulsive disorder. PLoS ONE 7, e36356.
Thesen, S., Heid, O., Mueller, E., Schad, L.R., 2000. Prospective acquisition correction for head motion with image-based tracking for real-time fMRI. Magn. Reson. Med. 44, 457–465.
Tien, A.Y., Pearlson, G.D., Machlin, S.R., Bylsma, F.W., Hoehn-Saric, R., 1992. Oculomotor performance in obsessive–compulsive disorder. Am. J. Psychiatry 149, 641–646.
Ursu, S., Stenger, V.A., Shear, M.K., Jones, M.R., Carter, C.S., 2003. Overactive action monitoring in obsessive–compulsive disorder: evidence from functional magnetic resonance imaging. Psychol. Sci. 14, 347–353.
Van Dijk, K.R., Hedden, T., Venkataraman, A., Evans, K.C., Lazar, S.W., Buckner, R.L., 2010. Intrinsic functional connectivity as a tool for human connectomics: theory, properties, and optimization. J. Neurophysiol. 103, 297–321.
Van 't Ent, D., Apkarian, P., 1999. Motoric response inhibition in finger movement and saccadic eye movement: a comparative study. Clin. Neurophysiol. 110, 1058–1072.
van Veen, V., Carter, C.S., 2002. The timing of action-monitoring processes in the anterior cingulate cortex. J. Cogn. Neurosci. 14, 593–602.
Vul, E., Pashler, H., 2012. Voodoo and circularity errors. Neuroimage 62, 945–948.
Vul, E., Harris, C., Winkielman, P., Pashler, H., 2009. Puzzlingly high correlations in fMRI studies of emotion, personality, and social cognition. Perspect. Psychol. Sci. 4, 274–290.
Wessel, J.R., Danielmeier, C., Ullsperger, M., 2011. Error awareness revisited: accumulation of multimodal evidence from central and autonomic nervous systems. J. Cogn. Neurosci. 23, 3021–3036.
White, K., Ashton, R., 1976. Handedness assessment inventory. Neuropsychologia 14, 261–264.
Wilkinson, G.J., 1993. The Wide Range Achievement Test — Revision 3. Jastak Associates, Wilmington, DE,.
Xiao, Z., Wang, J., Zhang, M., Li, H., Tang, Y., Wang, Y., Fan, Q., Fromson, J.A., 2011. Error-related negativity abnormalities in generalized anxiety disorder and obsessive–compulsive disorder. Prog. Neuro-Psychopharmacol. Biol. Psychiatry 35, 265–272.
Yeung, N., Botvinick, M.M., Cohen, J.D., 2004. The neural basis of error detection: conflict monitoring and the error-related negativity. Psychol. Rev. 111, 931–959.